ARTICLE

Check for updates

Journal of
Sensor Science and Technology

The Korean Sensors Society

Flexible Thermoelectric Energy Harvester based on Ionic Liquid-Incorporated $Bi_{0.5}Sb_{1.5}Te_3$-PVDF Composite Films

Hyejeong Choi[1,2,*], Jimin Lee[1,*], HakSu Jang[1,2,*], Nagamalleswara Rao Alluri[1,3], Jong Min Park[1], Wonho Choi[1,2], and Kwi-Il Park[1,2,3,+]

[1]*Department of Materials Science and Metallurgical Engineering, Kyungpook National University, Daegu, 41566, Republic of Korea*
[2]*Innovative Semiconductor Education and Research Center for Future Mobility, Kyungpook National University, 80 Daehak-ro, Buk-gu, Daegu, 41566, Republic of Korea*
[3]*Research Institute of Automotive Parts and Materials, Kyungpook National University, 80 Daehak-ro, Buk-gu, Daegu 41566, Republic of Korea*

Cite This: *J. Sens. Sci. Technol. Vol. 35, No. 2 (2026) 130-135*

https://doi.org/10.46670/JSST.2026.35.2.130

ABSTRACT: Thermoelectric (TE) composite films that can harvest electrical energy from ambient heat sources are attractive for flexible and battery-free power sources, yet their performance is often limited by unfavorable transport trade-offs in polymer-based composites. Here, we report an effective approach to enhance flexible TE films by incorporating an ionic liquid (IL) into a PVDF-based organic-inorganic composite containing p-type $Bi_{0.5}Sb_{1.5}Te_3$ (BST) powders. Composite solutions with different IL concentrations (3-20 wt%) were prepared and then drop-cast to produce free-standing TE films with a thickness of ~100 μm. Increasing the IL content enhanced the Seebeck coefficient but decreased the electrical conductivity, signifying IL-induced alterations in charge transport and interfacial scattering. An optimal IL content of 15 wt% produced the highest power factor of 3.22 μW $m^{-1}K^{-2}$, which is ≈1.45 times higher than that of a bare TE film. A flexible energy harvester fabricated by integrating IL-based TE films onto polyimide substrates delivered a maximum output power of 6.67 nW at ΔT = 20 K, corresponding to an ≈3.75-fold improvement compared to the IL-free devices. These results demonstrate IL-assisted tuning as an effective route toward conformal, self-powered wearable devices and sensor platforms.

KEYWORDS: *Ionic liquid, Ionic thermoelectric, Thermoelectric generator, Flexible, Energy harvesting*

1. INTRODUCTION

Thermoelectric (TE) materials have recently attracted attention as process-compatible platforms for flexible and battery-free power sources, since they can generate electrical output even under small temperature gradients (ΔT) via coupled ionic and electronic transport[1-4]. With the rapid proliferation of wireless communication networks and electronic devices, global energy consumption has increased dramatically, driving strong interest in energy harvesting technologies capable of scavenging energy from the ambient environment. Among these approaches, thermoelectric generators (TEGs) that harvest electricity from ambient heat sources have gained significant attention as a sustainable power solution, as they enable continuous electricity generation without batteries simply by maintaining a ΔT [5-8].

TEGs function through the Seebeck effect, in which a temperature difference (ΔT) across a material induces charge carrier diffusion, generating an electrical potential and electromotive force independent of device geometry. Owing to this principle, TEGs are applicable not only to wearable electronics but also to industrial and manufacturing environments where waste heat is ubiquitously generated. Their ability to convert small temperature differences into electrical energy makes them highly versatile for self-powered systems [5,9,10].

The performance of TE materials is quantified by the dimensionless figure of merit, zT, defined as $zT = S^2\sigma T/\kappa$, where S is the Seebeck coefficient, σ is the electrical conductivity, T is the absolute temperature, and κ is the thermal conductivity. Achieving a high zT requires a high

*These authors contributed equally to this work.
+Corresponding author: kipark@knu.ac.kr
Received : Mar. 6, 2026, Revised : Mar. 10, 2026, Accepted : Mar. 11, 2026

power factor ($S^2\sigma$) while simultaneously suppressing κ. However, the strong interdependence among these parameters imposes intrinsic limitations, making their simultaneous optimization challenging [11-14].

Bismuth telluride (Bi_2Te_3), a representative room-temperature TE material, exhibits excellent intrinsic TE performance but suffers from limited tunability due to the trade-off between σ and S, as well as poor mechanical flexibility and processability [14,15]. To overcome these limitations, recent studies have explored organic–inorganic TE composites incorporating polymers or ionic components to decouple transport properties and enable enhanced control over charge carrier behavior [16,17].

Ionic liquids (ILs) are a class of molten salts composed entirely of organic cations and inorganic or organic anions that remain in a liquid state at or near room temperature. Owing to their negligible vapor pressure, high thermal stability, and excellent ionic conductivity, ILs have been extensively investigated in electrochemical and energy-related applications. Furthermore, the wide tunability of cation–anion combinations enables precise control over physicochemical properties such as polarity, viscosity, and ion transport behavior [18-21].

Within the realm of TE materials, ILs have recently emerged as promising functional additives that can influence charge carrier transport and interfacial interactions. The incorporation of ILs can induce energy filtering effects, adjust carrier concentration through interfacial doping, and inhibit phonon transport via enhanced interfacial scattering, thereby offering a potential pathway to decouple the interdependent TE parameters (S, σ, and κ) [1,2,22-25]. These characteristics make ILs particularly attractive for hybrid organic–inorganic TEGs.

Herein, ILs were incorporated into a Bi_2Te_3-based TE system to facilitate efficient adjustment of charge transport and interfacial interactions, consequently enhancing TE performance while ensuring process compatibility [26,27]. PVDF-based TE composite films were prepared by adding p-type $Bi_{0.5}Sb_{1.5}Te_3$ (BST) powders as an inorganic filler and different quantities of ILs into a PVDF polymer matrix, followed by a drop-casting [28-31]. The TE properties of the prepared composite films, such as the Seebeck coefficient, electrical conductivity, and power factor, were assessed with a customized TE characterization system. A rise in both the Seebeck coefficient and power factor was noted with increasing IL content. The impact of IL inclusion in the film displayed saturation characteristics at 20 wt%, with an optimal formulation found at 15 wt%. Furthermore, the optimized TE composite films were cut to appropriate dimensions and integrated into flexible substrates to fabricate an IL-adopted TE generator (IL-TEG). The resulting IL-TEG generated a maximum output power of 6.67 nW under a ΔT of 20 K. Specifically, IL-TEG showed an output performance enhancement of approximately 3.75 times when compared to conventional PVDF-based IL-free TEGs. These findings indicate that the addition of IL is a successful strategy for improving the TE performance and power generation ability of flexible TEGs, implying their possible uses in wearable devices and surface-mounted sensing systems.

2. EXPERIMENTAL

2.1 Synthesis of ionic liquids

1-Bromohexyl-1-methylpiperidinium bromide (Br-6-MPRD) IL powder [32,33] was synthesized by quaternization of N-methylpiperidine (Sigma Aldrich, USA) with 1,6-dibromohexane (Sigma Aldrich, USA), as illustrated in Figs. 1(a) and 1(b). Initially, 9.5 mL (30.90 mmol) of 1,6-dibromohexane was mixed into 30 mL of ethyl acetate, and a uniform solution was obtained by stirring at room temperature for 5 min. Thereafter, 7.5 mL (20.51 mmol) of N-methylpiperidine was gradually added to the reaction mixture, which was allowed to react for 72 h at room temperature with constant stirring. Upon completion of the reaction, a white precipitate was formed and collected through filtration. The crude product was thoroughly washed with ethyl acetate to remove unreacted materials and residual impurities, and then dried under vacuum at room temperature to yield the final product. Fig. 1(b) shows the chemical reaction scheme for the synthesis of the Br-6-MPRD IL.

2.2 Fabrication of PVDF-based IL-incorporated TE composite films

A TE composite solution was prepared by dissolving PVDF (Kynar 2821-co, Arkema, South Korea) powder, BST powder

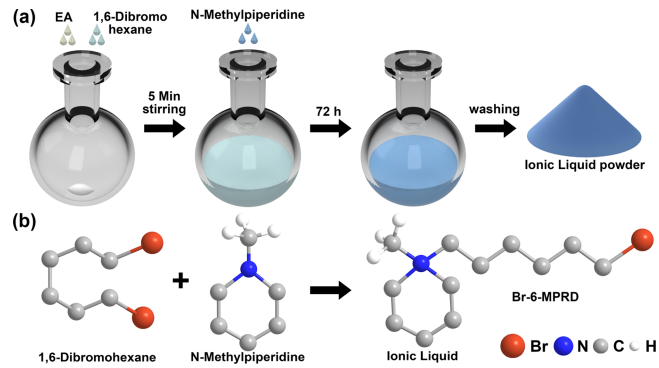

Fig. 1. (a) Schematic illustration of the synthesis procedure for the Br-6-MPRD IL powders. (b) Chemical reaction scheme for the synthesis of the IL.

(Hanaro TR. Co. Ltd, South Korea) and IL in a mixed solvent composed of acetone and N,N-dimethylformamide (DMF) at a 7:3 mass ratio under continuous stirring. Several homogeneous composite solutions were prepared by varying the IL concentration to 3, 7, 11, 15, and 20 wt% relative to the total weight of the composite. A specific quantity of TE BST filler particles was added to the PVDF polymer, as too much BST in PVDF could compromise film flexibility and cause surface roughness. Consequently, for all the composite films, the mass fraction of BST was kept constant at 75 wt% in relation to PVDF. Finally, the versatile PVDF-based TE composite films were produced by drop-casting the prepared composite solutions onto cleaned glass substrates, followed by drying in an oven at 80°C for 1 h.

2.3 Characterization of IL-adopted TE composite films

The IL formation and its chemical structure and bonding interactions were systematically characterized by FT-IR (PerkinElmer, Frontier, USA) and 500 MHz NMR spectroscopy (BRUKER, AvanceNeo500, USA). The crystalline phase and composition of the BST powder were analyzed through X-ray diffraction (XRD; Empyrean, PANalytical, China) utilizing Cu Kα radiation (λ = 1.5406 Å). The thickness and surface morphology of the TE composite films were examined using field emission scanning electron microscopy (FE-SEM, JSM-IT700HR, Japan). The TE properties of the fabricated composite films such as the S, σ, and power factor, were assessed utilizing a specially designed four-point probe–based TE measurement system. The system consists of a Peltier device for generating a controlled ΔT, a source meter (2612B, Keithley, USA), a multichannel measurement system (3706A, Keithley, USA), a nanovoltmeter (2182A, Keithley, USA), and a DC power supply (GPP-1326, GW Instek, Taiwan). The four probes were brought into direct contact with the TE film to simultaneously measure the ΔT and the TE voltage generated across the sample. The S and electrical conductance were simultaneously measured and recorded using a computer-based data acquisition system. The σ was calculated from the measured conductance by considering the probe spacing and the cross-sectional area of the TE film. The power factor was determined using the equation $PF = S^2\sigma$.

2.4 Fabrication of energy harvester based on IL-adopted TE films

A TEG was constructed by cutting the PVDF-based IL-adopted TE composite films into rectangular pieces (2×0.5 cm^2) and affixing them to a flexible polyimide (PI) substrate (3×5.5 cm^2) using conductive epoxy (CW2400, Chemtronics Co. Ltd, South Korea). Electrical connections linking the TE films to the electrodes were established using aluminum foil and conductive epoxy, providing a consistent contact area of 5×5 mm^2 between each TE element and the electrodes. Copper wires were connected to both ends of the electrodes with conductive epoxy to collect the output voltage and current produced by the TE energy harvester.

2.5 Evaluation of output performance harvested from an IL-TEG

A custom measurement system was developed to assess the electrical output of the flexible IL-TEG. A temperature gradient was controlled across the TE element by heating one side with a hot plate (MSH20D, Daihan Scientific, South Korea) and cooling the other side with a chiller (RW3-3025, Lab Companion, South Korea). The ΔT across the TEG was monitored continuously with a digital contact thermometer (A1.T9214T, Daihan Scientific, South Korea). Load resistance analysis for the IL-TEG was conducted by varying the load resistance from 100 Ω to 1 MΩ using a resistance box (RS-200W, IET Labs, Inc., USA), while the output voltage and current were measured with a source meter (2612B, Keithley, USA). The output power ($P = V \times I$) of the harvester was calculated using the measured voltage and current.

3. RESULTS AND DISCUSSIONS

3.1 Chemical structure analysis of Br-6-MPRD IL

The chemical structure and its bond formation of the Br-6-MPRD IL were confirmed by ^{1}H NMR, as shown in Fig. 2(a) [32,33]. The characteristic resonance peak at 3.10 ppm relates to the methyl protons of the piperidinium ring,while the peak at 3.70 ppm pertains to the methylene protons adjacent to the nitrogen cation. The peaks observed in the range of 1.97 to 1.99 ppm were assigned to the remaining CH_2 groups on the piperidine ring, while the resonance peaks at 1.80, 1.45, and 1.21 ppm correspond to the methylene protons of the alkyl spacer. In addition, the peak at 3.35 ppm is related to the methylene protons in the aliphatic chain adjacent to the bromine atom. FT-IR spectroscopy further confirmed the current chemical structure and detailed information regarding the chemical bonds of the Br-6-MPRD IL, as shown in Fig. 2(b) [32,33]. The absorption bands located at 2860 and 2940 cm^{-1} correspond to the C-H stretching vibrations of alkyl chains, whereas the band at 1468 cm^{-1} is associated with the C-H bending vibrations of Br-6-MPRD. The broad absorption band at 3400 cm^{-1} is attributed to O-H stretching related to

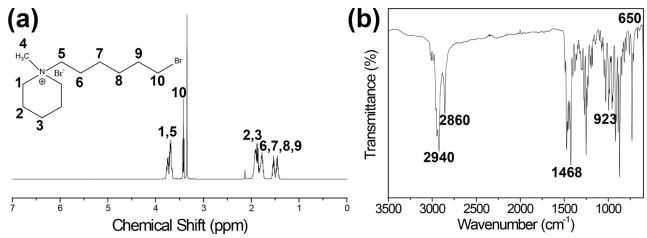

Fig. 2. Spectroscopic characterization of the Br-6-MPRD IL: (a) ^{1}H NMR spectrum and (b) FT-IR spectrum.

moisture adsorbed onto the IL. Furthermore, the characteristic absorption band at 923 cm^{-1} is correlated with the C-N^{+} stretching vibration of the piperidinium group, verifying the formation of the quaternary ammonium structure.

3.2 IL-adopted TE films and flexible IL-TEGs

Fig. 3(a) illustrates the fabrication process of the flexible IL-adopted TE composite films utilizing different composite solutions with varying IL concentrations, specifically 3, 7, 11, 15, and 20 wt%. Detailed information on the film processing conditions is provided in the Experimental section. Fig. 3(b) shows an optical image of the as-prepared final TE composite film. Fig. 3(c) depicts the fabrication steps of the flexible TEG using the IL-adopted TE composite film. The TE composite film was affixed to a flexible PI substrate and electrically interconnected using aluminum foil, ensuring reliable electrical contact while maintaining the composite film's mechanical flexibility. Fig. 3(d) shows the optical image of the IL-TEG, whose flexibility was validated by bending it by hand. This indicates strong mechanical compliance, suggesting that the TEG is a promising candidate for the wearable and surface-mounted sensing and energy harvesting applications.

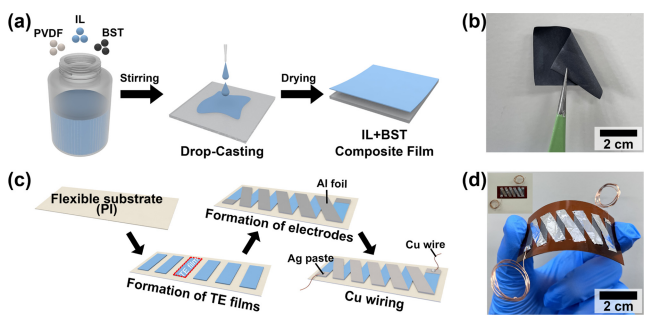

Fig. 3. (a) Schematic illustration of the fabrication process for the flexible TE composite films. (b) Optical photograph of the fabricated IL-adopted TE film. (c) Schematic diagram showing the fabrication procedure for the flexible IL-TEG. (d) Photograph of the device bent by hand.

3.3 TE properties of IL-adopted TE composite films

Fig. 4(a) shows the cross-sectional SEM image of the TE composite film, revealing a thickness of approximately 100 μm. The surface morphology of the TE composite film verifies the presence of the BST powder and its uniform distribution within the PVDF polymer matrix (Fig. 4(b)). Fig. 4(c) shows the XRD pattern of the BST powder as the TE filler used to fabricate TE film, which aligns well with the standard JCPDS reference (#49-1713), affirming the high purity of its crystalline phase. Figs. 4(d) and 4(e) show the Seebeck coefficient and electrical conductivity of the TE composite films relative to IL content, respectively; these results were evaluated with a four-point probe-based TE characterization system. The observed increase in the Seebeck coefficient accompanied by a reduction in electrical conductivity indicates that IL incorporation redirects TE transport towards a Seebeck-dominant regime. This behavior is often linked to energy-filtering effects and increased carrier scattering at ionic and polymer–inorganic interfaces, emphasizing the importance of ILs in selectively tuning charge transport characteristics. The incorporation of the IL is anticipated to increase the free volume in the PVDF polymer matrix, resulting in adjusted polymer chain arrangements and modulated charge carrier transport. Fig. 4(f) shows the power factor of the flexible TE composite films as a function of IL concentration in polymer. The power factor of the TE composite films increased as the IL concentration changed from 3 to 15 wt%. The maximum power factor of 3.22 μW m^{-1} K^{-2} was achieved at an IL content of 15 wt%, which is approximately 1.45 times greater than that of the pristine PVDF-based TE film. These findings indicate that the inclusion of ILs in TE composite films is an effective strategy for enhancing TEG performance.

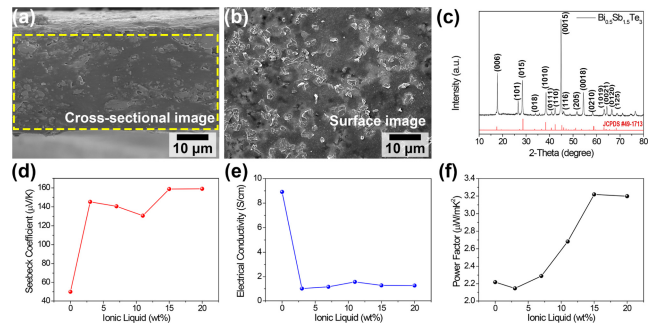

Fig. 4. (a, b) Cross-sectional (a) and surface SEM images (b) of the IL-adopted TE composite film. (c) An XRD pattern of the p-type BST TE powder compared with the standard JCPDS pattern. (d-f) TE properties of the fabricated composite films as a function of IL concentration: (d) Seebeck coefficient, (e) electrical conductivity, and (f) power factor.

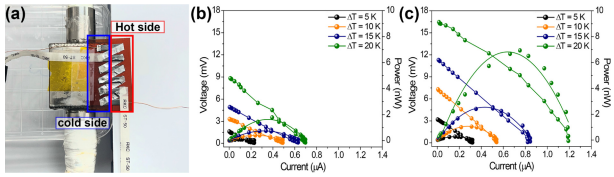

Fig. 5. (a) Optical image of the custom measurement system with a TEG for evaluating its output performance. (b, c) Voltage-current-power curves of the flexible TEGs fabricated by IL-free (b) and IL-adopted TE (c).

3.4 Energy harvesting performance of an IL-TEG

Fig. 5(a) shows an optical image of the measurement system with an IL-TEG for demonstrating the energy harvesting. By introducing a controlled ΔT across the device using a hot plate and a chiller unit, the output signals such as load voltage and current values were simultaneously detected. A detailed description of the measurement setup is provided in the Experimental section. Figs. 5(b) and 5(c) compare the power generation performance of TEGs utilizing composite films made with and without the adoption of IL. The TEG based on the pristine TE composite film produced a maximum voltage of 0.69 mV, a maximum current of 8.83 μA, and a maximum output power of approximately 1.78 nW at the $\Delta T = 20$ K. In contrast, the IL-TEG generated a maximum output voltage of 1.09 mV, a maximum current of 16.45 μA, and a maximum output power of approximately 6.67 nW at the same ΔT. Overall, the output response of the IL-TEG was significantly greater than that of the conventional IL-free TEG, demonstrating that the inclusion of ILs in the system decreases the electrical conductivity of the composite film while improving the charge carrier mobility within the device.

4. CONCLUSIONS

In summary, flexible TE composite films were produced by varying the IL concentration in the BST-PVDF composite solution. The IL-adopted TE composite film exhibited a power factor of 3.22 μW m^{-1} K^{-2} when the IL concentration was 15 wt%, which represents a 1.45-fold enhancement compared to the IL-free film. Additionally, the impact of the IL on TEG performance was assessed systematically and compared with the output of the IL-free device. The IL-TEG with an IL content of 15 wt% produced a maximum output power of 6.67 nW at $\Delta T = 20$ K, which is approximately 3.75 times greater than that of the IL-free device. These results indicate that the incorporation of ILs is an effective strategy for enhancing the energy conversion efficiency of TE composite films and boosting the power generation ability of flexible TEGs, highlighting their potential for use in conformal wearable electronics and surface-mounted sensing platforms.

CRediT Authorship Contribution Statement

Hyejeong Choi: Writing – original draft, Data curation, Methodology, Experiment, Conceptualization. **Jimin Lee:** Experiment, Data curation. **HakSu Jang:** Data curation, Formal analysis, Validation. **Nagamalleswara Rao Alluri**: Writing – review & editing. **Jong Min Park**: Writing – review & editing. **Wonho Choi**: Methodology, Writing – review & editing. **Kwi-Il Park:** Writing - review & editing, Funding acquisition, Supervision.

Declaration of Competing Interest

The authors declare that they have no known competing financial interests or personal relationships that could have appeared to influence the work reported in this paper.

Acknowledgements

This work was supported by the National Research Foundation of Korea (NRF) grant funded by the Korea government (MSIT) (No. RS-2022-NR069105 and No. RS-2024-00403822).

REFERENCES

[1] S. Sun, M. Li, X.L. Shi, Z.G. Chen, Advances in ionic thermoelectrics: from materials to devices, Adv. Energy Mater. 13 (2023) 2203692.
[2] M.A. Okirigiti, K.-I. Park, Flexible Thermoelectric Materials for Wearable Energy Harvesting: Advances in Polymers and Hybrid Architectures, J. Electr. Electron. Mater. 38 (2025) 469–480.
[3] D. Song, C. Zhao, B. Chen, W. Ma, K. Wang, X. Zhang, Conveyor mode enabling continuous ionic thermoelectric conversion, Joule 8 (2024) 3217–3232.
[4] H. Jeon, C.M. Kim, H.J. Park, B. Bae, H. Choi, H. Jang, et al., Flexible Hybrid Energy Harvester based Thermoelectric Composite Film and Electrospun Piezopolymer Membranes, J. Powder Mater. 32 (2025) 104–112.
[5] M. Massetti, F. Jiao, A.J. Ferguson, D. Zhao, K. Wijeratne, A. Würger, et al., Unconventional thermoelectric materials for energy harvesting and sensing applications, Chem. Rev. 121 (2021) 12465–12547.
[6] M.A. Okirigiti, C.M. Kim, H. Choi, N.R. Alluri, C. Baek, M.-K. Lee, et al., Enhanced energy harvesting performance of bendable thermoelectric generator enabled by trapezoidal-shaped legs, J. Power Sources 631 (2015) 23625.
[7] S. Kim, Y. Na, C. Nam, C.K. Jeong, K.T. Kim, K.-I. Park, Highly tailorable, ultra-foldable, and resorbable thermoelectric paper for origami-enabled energy generation, Nano Energy 103 (2022) 107824.
[8] S. Kim, D.Y. Hyeon, D. Lee, J.H. Bae, K.-I. Park, Fully

flexible thermoelectric and piezoelectric hybrid generator based on a self-assembled multifunctional single composite film, Mater. Today Phys. 35 (2023) 101103.
[9] W. Zhou, K. Yamamoto, A. Miura, R. Iguchi, Y. Miura, K.-i. Uchida, et al., Seebeck-driven transverse thermoelectric generation, Nat. Mater. 20 (2021) 463–467.
[10] C.-T. Hsu, G.-Y. Huang, H.-S. Chu, B. Yu, D.-J. Yao, An effective Seebeck coefficient obtained by experimental results of a thermoelectric generator module, Appl. Energy 88 (2011) 5173–5179.
[11] L. Yang, Z.G. Chen, M.S. Dargusch, J. Zou, High performance thermoelectric materials: progress and their applications, Adv. Energy Mater. 8 (2018) 1701797.
[12] J. Wei, L. Yang, Z. Ma, P. Song, M. Zhang, J. Ma, et al., Review of current high-ZT thermoelectric materials, J. Mater. Sci. 55 (2020) 12642–12704.
[13] Z. Ma, J. Wei, P. Song, M. Zhang, L. Yang, J. Ma, et al., Review of experimental approaches for improving zT of thermoelectric materials, Mater. Sci. Semicond. Process. 121 (2021) 105303.
[14] L.Y. Lou, J. Yang, Y.K. Zhu, H. Liang, Y.X. Zhang, J. Feng, et al., Tunable electrical conductivity and simultaneously enhanced thermoelectric and mechanical properties in n-type Bi_2Te_3, Adv. Sci. 9 (2022) 2203250.
[15] X. Tang, Z. Li, W. Liu, Q. Zhang, C. Uher, A comprehensive review on Bi_2Te_3-based thin films: thermoelectrics and beyond, Interdiscip. Mater. 1 (2022) 88–115.
[16] L. Wang, Z. Zhang, Y. Liu, B. Wang, L. Fang, J. Qiu, et al., Exceptional thermoelectric properties of flexible organic–inorganic hybrids with monodispersed and periodic nanophase, Nat. Commun. 9 (2018) 3817.
[17] H. Jin, J. Li, J. Iocozzia, X. Zeng, P.C. Wei, C. Yang, et al., Hybrid organic–inorganic thermoelectric materials and devices, Angew. Chem. Int. Ed. 58 (2019) 15206–15226.
[18] Y. Pei, Y. Zhang, J. Ma, M. Fan, S. Zhang, J. Wang, Ionic liquids for advanced materials, Mater. Today Nano 17 (2022) 100159.
[19] D.D. Patel, J.M. Lee, Applications of ionic liquids, Chem. Rec. 12 (2012) 329–355.
[20] L. Zhang, X. Fu, G. Gao, Anion–cation cooperative catalysis by ionic liquids, ChemCatChem 3 (2011) 1359–1364.
[21] T. Zhou, C. Gui, L. Sun, Y. Hu, H. Lyu, Z. Wang, et al., Energy applications of ionic liquids: recent developments and future prospects, Chem. Rev. 123 (2023) 12170–12253.
[22] H. Wang, D. Zhao, Z.U. Khan, S. Puzinas, M.P. Jonsson, M. Berggren, et al., Ionic thermoelectric figure of merit for charging of supercapacitors, Adv. Electron. Mater. 3 (2017) 1700013.
[23] H. Keppner, S. Uhl, E. Laux, L. Jeandupeux, J. Tschanz, T. Journot, Ionic Liquid-based thermoelectric generator: links between liquid data and generator characteristics, Mater. Today Proc. 2 (2015) 680–689.
[24] T.J. Abraham, D.R. MacFarlane, J.M. Pringle, Seebeck coefficients in ionic liquids–prospects for thermo-electrochemical cells, Chem. Commun. 47 (2011) 6260–6262.
[25] W.D. Gonçalves, C. Caspers, J. Dupont, P. Migowski, Ionic liquids for thermoelectrochemical energy generation, Curr. Opin. Green Sustain. Chem. 26 (2020) 100404.
[26] J. Szymczak, S. Legeai, S. Michel, S. Diliberto, N. Stein, C. Boulanger, Electrodeposition of stoichiometric bismuth telluride Bi_2Te_3 using a piperidinium ionic liquid binary mixture, Electrochim. Acta 137 (2014) 586–594.
[27] K.-C. Kim, S.-H. Baek, H.J. Kim, D.-B. Hyun, S.K. Kim, J.-S. Kim, Thermopower enhancement of Bi_2Te_3 films by doping I ions, J. Electron. Mater. 43 (2014) 2000–2005.
[28] Y. Na, S. Kim, S.P.R. Mallem, S. Yi, K.T. Kim, K.-I. Park, Energy harvesting from human body heat using highly flexible thermoelectric generator based on Bi_2Te_3 particles and polymer composite, J. Alloys Compd. 924 (2022) 166575.
[29] R. Mori, Y. Mayuzumi, M. Yamaguchi, A. Kobayashi, Y. Seki, M. Takashiri, Improved thermoelectric properties of solvothermally synthesized Bi_2Te_3 nanoplate films with homogeneous interconnections using Bi_2Te_3 electrodeposited layers, J. Alloys Compd. 818 (2020) 152901.
[30] I. Imae, H. Uehara, K. Imato, Y. Ooyama, Thermoelectric properties of conductive freestanding films prepared from PEDOT: PSS aqueous dispersion and ionic liquids, ACS Appl. Mater. Interfaces 14 (2022) 57064–57069.
[31] Z. Li, L. Deng, H. Lv, L. Liang, W. Deng, Y. Zhang, et al., Mechanically robust and flexible films of ionic liquid-modulated polymer thermoelectric composites, Adv. Funct. Mater. 31 (2021) 2104836.
[32] V. Vijayakumar, J.H. Kim, S.Y. Nam, Piperidinium functionalized poly (2, 6 dimethyl 1, 4 phenylene oxide) based polyionic liquid/ionic liquid (PIL/IL) composites for CO2 separation, J. Ind. Eng. Chem. 99 (2021) 81–89.
[33] H.S. Jang, H.N. Jeong, S.M. Eom, S.M. Han, S.H. Kim, H.W. Kwon, et al., Robust anion exchange membranes based on ionic liquid grafted chitosan/polyvinyl alcohol/quaternary ammonium functionalized silica for polymer electrolyte membrane fuel cells, Int. J. Biol. Macromol. 262 (2024) 129979.